European Journal of Medicinal Chemistry 182 (2019) 111610

Contents lists available at ScienceDirect

European Journal of Medicinal Chemistry

journal homepage: http://www.elsevier.com/locate/ejmech

Research paper

Synthesis, structure-activity relationship and trypanocidal activity of pyrazole-imidazoline and new pyrazole-tetrahydropyrimidine hybrids as promising chemotherapeutic agents for Chagas disease

M.E. Monteiro [a, 1], G. Lechuga [a, 1], L.S. Lara [a, 1], B.A. Souto [b], M.G. Viganó [b], S.C. Bourguignon [c], C.M. Calvet [a], F.O.R. Oliveira Jr. [a], C.R. Alves [d], F. Souza-Silva [d, e], M.S. Santos [b, **], M.C.S. Pereira [a, *]

[a] Laboratório de Ultraestrutura Celular, Instituto Oswaldo Cruz, Fiocruz, Av. Brasil 4365 Manguinhos, 21040-900, Rio de Janeiro, RJ, Brazil
[b] Laboratório de Síntese Orgânica (LABSINTO), Instituto de Física e Química, Universidade Federal de Itajubá, Avenida BPS, 1303, Pinheirinho, Itajubá, 37500-903, Minas Gerais, Brazil
[c] Laboratório de Interação Celular e Molecular, Departamento de Biologia Celular e Molecular, Universidade Federal Fluminense, Rua Outeiro São João Batista, 24020-141, Niterói, Rio de Janeiro, Brazil
[d] Laboratório de Biologia Molecular e Doenças Endêmicas, Instituto Oswaldo Cruz, Fiocruz, Av. Brasil 4365 Manguinhos, 21040-900, Rio de Janeiro, RJ, Brazil
[e] Centro de Desenvolvimento Tecnológico em Saúde, Fiocruz, Avenida Brasil 4365, Manguinhos, 21040-900, Rio de Janeiro, RJ, Brazil

ARTICLE INFO

Article history:
Received 20 March 2019
Received in revised form
8 August 2019
Accepted 9 August 2019
Available online 10 August 2019

Keywords:
Chagas disease
Trypanosoma cruzi
Chemotherapy
Pyrazolederivatives
Cruzipain inhibitor
SAR analysis

ABSTRACT

Drug therapy for Chagas disease remains a major challenge as potential candidate drugs have failed clinical trials. Currently available drugs have limited efficacy and induce serious side effects. Thus, the discovery of new drugs is urgently needed in the fight against Chagas' disease. Here, we synthesized and evaluated the biological effect of pyrazole-imidazoline (1a-i) and pyrazole-tetrahydropyrimidine (2a-i) derivatives against relevant clinical forms of *Trypanosoma cruzi*. The structure-activity relationship (SAR), drug-target search, physicochemical and ADMET properties of the major active compounds *in vitro* were also assessed *in silico*. Pyrazole derivatives showed no toxicity in Vero cells and also no cardiotoxicity. Phenotypic screening revealed two dichlorinated pyrazole-imidazoline derivatives (1**c** and 1**d**) with trypanocidal activity higher than that of benznidazole (Bz) against trypomastigotes; these were also the most potent compounds against intracellular amastigotes. Replacement of imidazoline with tetrahydropyrimidine in the pyrazole compounds completely abolished the trypanocidal activity of series 2(**a-i**) derivatives. The physicochemical and ADMET properties of the compounds predicted good permeability, good oral bioavailability, no toxicity and mutagenicity of **1c** and **1d**. Pyrazole nucleus had high frequency hits for cruzipain in drug-target search and structure activity relationship (SAR) analysis of pyrazole-imidazoline derivatives revealed enhanced activity when chlorine atom was inserted in *meta*-positions of the benzene ring. Additionally, we found evidence that both compounds (1**c** and 1**d**) have the potential to interact non-covalently with the active site of cruzipain and also inhibit the cysteine proteinase activity of *T. cruzi*. Collectively, the data presented here reveal pyrazole derivatives with promise for further optimization in the therapy of Chagas disease.

1. Introduction

Chagas disease (CD), a silent disease caused by *Trypanosoma cruzi*, is a serious global public health problem [1]. CD is endemic in 21 countries of Latin America, with a prevalence of 62% of cases (3,5 million) in countries of the Southern Cone [2]. The expansion of its geographical distribution to non-endemic regions is related to emigration of infected individuals [3]. Mild symptoms or no medical problems are mostly observed in the acute phase of the disease,

* Corresponding author.
** Corresponding author.
E-mail addresses: mauriciosantos@unifei.edu.br (M.S. Santos), mirian@ioc.fiocruz.br (M.C.S. Pereira).
[1] These authors contributed equally to the work.

https://doi.org/10.1016/j.ejmech.2019.111610
0223-5234/

whereas the chronic phase may have a silent clinical course which progresses ultimately to serious cardiac or gastrointestinal complications [4]. Negligence in the diagnosis and treatment of the disease contributes to high morbidity and mortality, since it is estimated that 80% of affected individuals do not have access to treatment [5]. Additionally, the lack of public policies to eradicate transmission in Latin America, where few countries have policies in place to control vectorial and transfusional transmission and provide health-care access to the at-risk population, are obstacles to attaining World Health Organization (WHO) 2020 goals to control CD [6,7].

The etiological treatment is still based on two nitroaromatic heterocycle compounds, benznidazole and nifurtimox, introduced more than 50 years ago, which have both low efficacy in the chronic phase and serious adverse effects. So far, little success has been achieved in drug discovery and development due to failure of potential azole-based candidates and combination therapy [8]. Posaconazole monotherapy resulted in therapeutic failure [9]. The STOP-CHAGAS trial demonstrated the trypanostatic action of posaconazole but no advantage over combined treatment with benznidazole (Bz), and showed lower efficacy than Bz monotherapy [10]. Furthermore, the Benznidazole Evaluation for Interrupting Trypanosomiasis (BENEFIT) trial also revealed that Bz was unable to prevent the progression of cardiomyopathy [11]. New clinical trials to improve drug safety and effectiveness are underway, including (i) Benznidazole New Doses Improved Treatment and Associations (BENDITA), which focuses on different therapeutic regimens of Bz as well as combinations of Bz with E1224, and (ii) Fexinidazole (FEXI12), also based on low dose and short duration treatment schedules (DNDi 2018) [12]. The current scenario for drug discovery for Chagas disease emphasizes the challenges of finding effective new drugs to combat this neglected disease.

Pyrazole is a five-membered aromatic heterocyclic ring containing two adjacent nitrogen atoms. It is found in many compounds with biological activity, including anti-inflammatory, antidepressant, anticancer, analgesic, antioxidant, antifungal, antiviral and antileishmanial drugs [13–16]. The potent pharmacological properties of nitrogen-containing heterocyclic compounds have stimulated efforts to design, synthesize and screen compounds containing a pyrazole nucleus against many infectious agents [16–19]. Microbicidal activity against pathogenic bacteria by coumarin-pyrazole carboxamide derivatives, a topoisomerase II and IV inhibitor, was higher than strong antibiotics such as novobiocin and ciprofloxacin [20]. Potent antimalarial activity, including against parasites resistant to currently used antimalarials, has been shown by pyrazoleamide derivatives, whose mechanism of action involves the disruption of Na^+ regulation [21]. Anti-trypanosomatid activity of some pyrazole derivatives has been reported to inhibit iron superoxide dismutase (Fe-SOD), disturbing antioxidant defense of the parasites [22].

We also drew attention to imidazoline and tetrahydropyrimidine. Both heterocyclic systems can be found in pharmacological compounds used to treat hyperglycemia, psychiatric disorders, cancer and bacterial infections [23,24]. Trypanocidal activity has also been reported for imidazoline and tetrahydropyrimidine derivatives. N-hydroxy imidazoline derivatives have demonstrated potent activity against *Trypanosoma brucei* in central nervous system stage (late-stage) sleeping sickness [25]. A pentamidine-related imidazoline series has also been evaluated against *T. brucei*, showing growth inhibition of the pentamidine-resistant isolates [26]. However, pyrazole-imidazoline and pyrazole-tetrahydropyrimidine hybrids have not yet been evaluated against Trypanosoma species. The only work relating to the pyrazole-imidazoline system was published by Santos and coworkers [27], in which an *in vitro* leishmanicidal effect against *Leishmania (L.) amazonensis* was demonstrated. The compound 5-amino-1-(3,5-dichlorophenyl)-4-(4,5-dihydro-1*H*-imidazol-2-yl)-1*H*-pyrazole showed a reduction of cutaneous lesion in *Leishmania (L.) amazonensis*-infected mice [27].

The promising activity of pyrazole, imidazoline and tetrahydropyrimidine led us to synthetize a series of 5-amino-1-aryl-4-(4,5-dihydro-1*H*-imidazol-2-yl)-1*H*-pyrazoles and 2-(-5-amino-1-aryl-1*H*-pyrazol-4-yl)-1,4,5,6-tetrahydropyrimidines to evaluate their trypanocidal activity as well as to investigate the structure-activity relationship. Together, the data we generated and report here revealed the effect of pyrazole-imidazoline derivatives as inhibitors of cysteine protease with anti-*T. cruzi* activity, highlighting their potential as hit compounds for treatment of Chagas disease.

2. Results and discussion

2.1. Chemical synthesis of compounds

The synthesis of the compounds 5-amino-1-aryl-4-(4,5-dihydro-1*H*-imidazol-2-yl)-1*H*-pyrazoles **1(a–i)** and 2-(-5-amino-1-aryl-1*H*-pyrazol-4-yl)-1,4,5,6-tetrahydropyrimidines **2(a–i)** is summarized in Scheme 1. In the first step, arylhydrazine hydrochlorides **3(a–i)** were unprotonated with sodium acetate in ethanol, under reflux, for 20 min. Then ethoxymethylenemalononitrile was added and the reaction was kept under reflux for 1 h to obtain 5-amino-1-aryl-1*H*-pyrazole-4-carbonitriles **4(a–i)** [28]. These key intermediates **4(a–i)** were the raw materials to access the targets **1(a–i)** and **2(a–i)** from 1,2-diaminoethane (ethylenediamine) and 1,3-diaminopropane, respectively, using carbon disulfide (CS_2) as catalyst [27]. All **2(a–i)** derivatives are published for the first time as well as compounds **1e**, **1f** and **1i**.

2.2. Biological activity of the pyrazole-imidazoline *1(a–i)* and pyrazole-tetrahydropyrimidine *2(a–i)* derivatives

Both series of synthetic compounds, pyrazole-imidazoline **1(a–i)** and pyrazole-tetrahydropyrimidine **2(a–i)** derivatives, were evaluated for cytotoxicity in Vero cells. Metabolic active cells were determined by quantitating the amount of ATP as an indicator of cell viability. All derivatives showed no toxicity in Vero cells (Tables 1 and 2; concentration of compound that reduces 50% of mammalian cell viability - CC_{50}) but the compounds of the pyrazole-imidazoline **1c** (257.1 ± 22.7 μM), **1d** (243.9 ± 51.6 μM) and **1h** (352.2 ± 43.4 μM), showed lower CC_{50} values than pyrazole-tetrahydropyrimidine **2c**, **2d** and **2h** analogs (CC_{50} > 500 μM). The *in vitro* phenotypic screening of **1(a–i)** and **2(a–i)** derivatives was performed on parasite forms relevant to human infection (trypomastigotes and intracellular amastigotes) (Tables 1 and 2). The biological activity, evaluated on bloodstream and culture-derived trypomastigote forms of *T. cruzi* Y strain and Dm28c-Luc clone, respectively, revealed a greater activity of the most active compounds **1c** (IC_{50} = 9.5 ± 1.2 μM) and **1d** (IC_{50} = 10.5 ± 1.1 μM) against *T. cruzi* Dm28c-Luc clone when compared to *T. cruzi* Y strain (**1c** - IC_{50} = 30.9 ± 1.1 μM and **1d** – IC_{50} = 28.3 ± 2.7 μM) and also to other analogs of the pirazole-imidazoline series against both *T. cruzi* stocks and Bz (Dm28c-Luc - IC_{50} = 19.1 ± 3.3 μM; Y - IC_{50} = 23.3 ± 4.5), the reference drug (Table 1). Additionally, **1c** (28.9 ± 1.6 μM) and **1d** (29.0 ± 2.3 μM) were 3.2-fold more effective than Bz (94.1 ± 5.3 μM) at IC_{90} level (Table 1).

The effect of the pyrazole-imidazoline derivatives was also evaluated against intracellular amastigotes. Three compounds of the series, **1b** (IC_{50} = 20.6 ± 1.7 μM), **1c** (IC_{50} = 16.5 ± 1.6 μM) and **1d** (IC_{50} = 13.7 ± 1.5 μM), showed moderate activity against intracellular forms of *T. cruzi* Dm28c-Luc clone (SI ≥ 15) while Bz was more

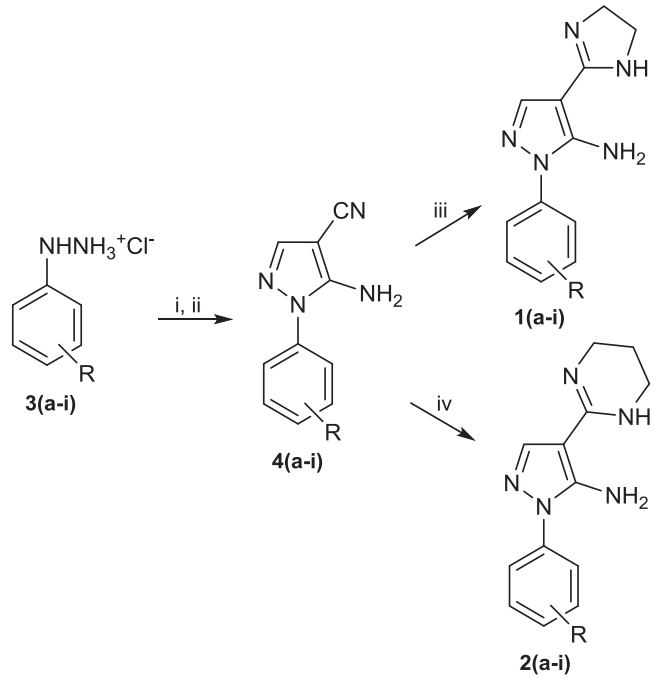

a: R=H; **b**: R=3-Cl; **c**: R=3,5-diCl; **d**: R=3,4-diCl; **e**: R=4-Cl; **f**: R=4-F; **g**: R=4-Br; **h**: R=3-Br; **i**: R=4-OCH_3.

Scheme 1. Reagents and conditions: i) sodium acetate, ethanol, 20 min, reflux; ii) ethoxymethylenemalononitrile, 1h, reflux; iii) 1,2-diaminoethane, CS_2, 12–14 h, 110–115 °C; iv) 1,3-diaminopropane, CS_2, 14–16 h, 85–95 °C.

Table 1
Cytotoxicity and trypanocidal effect of pyrazole derivatives.

Compounds	Trypanocidal effect (mean ± SD μM)						Vero cells toxicity CC_{500} (mean ± SD μM)	Selectivity index (SI)		
	Trypomastigotes				Intracellular amastigote Dm28c-Luc			Trypomastigotes		Intracellular amastigote Dm28c-Luc
	Dm28c-Luc		Y strain					Dm28c-Luc	Y strain	
	IC_{50}	IC_{90}	IC_{50}	IC_{90}	IC_{50}	IC_{90}				
1a	>100	>100	>100	>100	84.2 ± 11.1	>100	>500	nd	nd	>5.9
1b	53.3 ± 4.2	81.1 ± 7.5	31.3 ± 1.9	>100	20.6 ± 1.7	55 ± 3.7	>500	9.4	>15.9	>24.3
1c	9.5 ± 1.2*	28.9 ± 1.6*	30.9 ± 1.9	>100	16.5 ± 1.6	29.9 ± 0.5	257.1 ± 22.7	27.1	8.3	15.6
1d	10.5 ± 1.1*	29.0 ± 2.3*	28.3 ± 2.7	>100	13.6 ± 1.5	30.5 ± 1.2	243.9 ± 51.6	23.3	8.6	17.9
1e	78.9 ± 9.3	>100	84.2 ± 7.7	>100	>100	>100	>500	>6.3	>5.9	nd
1f	>100	>100	>100	>100	>100	>100	>500	nd	nd	nd
1g	>100	>100	52.3 ± 1.0	>100	84.2 ± 5.4	>100	>500	nd	>9.5	>5.9
1h	>100	>100	27.7 ± 1.6	>100	67.4 ± 6.7	>100	352.2 ± 43.4	nd	12.7	5.2
1i	>100	>100	>100	>100	63.4 ± 3.5	>100	>500	nd	nd	>7.9
2(a-i)	>100	>100	>100	>100	>100	>100	>500	nd	nd	nd
Bz	19.1 ± 3.3	94.1 ± 5.3	23.3 ± 4.5	>100	1.9 ± 0.2	6.9 ± 0.4	>500	>26.3	>21.4	>263.1

Average values of three independent experiments ± standard deviations; (*) Student *t*-test (*) $p \leq 0.001$.
IC_{50} and IC_{90}: concentration that produces 50% and 90% inhibitory effect, respectively. CC_{50}: concentration that reduce 50% of Vero cells viability.
SI = CC_{50} Vero cells/IC_{50} Trypomastigotes and intracellular amastigote forms of *T.* cruzi.
nd = Not determined.
SD = Standard deviations.

Table 2
Cardiotoxic effect and trypanocidal activity of pyrazole-imidazoline analogs and Bz.

Compounds	Intracellular amastigote Y strain (IC_{50} μM)	Toxicity in cardiomyocytes (CC_{50} μM)	SI
Bz	0.9 ± 0.1	>500	>555
1c	12.5 ± 1.1	378.9 ± 12.1	30.3
1d	12.7 ± 0.7	411.5 ± 23.7	32.4

Average values of three independent experiments ± standard deviations.
CC_{50}: concentration that reduce 50% of cardiomyocyte viability.
Selectivety index (SI) = CC_{50} Cardiomyocytes/IC_{50} intracellular amastigote forms of *T. cruzi*.

effective ($IC_{50} = 1.9 \pm 0.2$ μM; SI > 263.1) (Table 1). At IC_{90} level, the **1c** (29.9 ± 0.5 μM) and **1d** (30.5 ± 1.2 μM) remained the most effective compounds of the pyrazole-imidazoline series, but still 4.4-fold less active than Bz (6.9 ± 0.4 μM) (Table 1).

The most active compounds of pyrazole-imidazoline series were selected to evaluate cardiotoxic effect and their activity against *T. cruzi* amastigotes Y strain. To assess the cardiotoxic potential of the compounds, primary cultures of cardiac muscle cells were treated for 72 h with **1c** and **1d** derivatives. The results revealed no cardiotoxicity showing CC_{50} values of 378.9 ± 12.1 μM and 411.5 ± 23.7 μM, for **1c** and **1d**, respectively (Table 2). A selective effect against intracellular amastigotes (SI ≥ 30), *T. cruzi* Y strain, was observed on both derivatives, reaching a 50% of effective dose at 12.5 ± 1.1 μM and 12.7 ± 0.7 μM for **1c** and **1d**, respectively (Table 2). An interesting observation is that the *in vitro* leishmanicidal activity of the **1c** derivative, which has similar potency ($IC_{50} = 15.5 \pm 6.8$ μM) against *Leishmania (L.) amazonensis* promastigotes forms, is still effective in reducing the cutaneous lesion *in vivo* [27]. These data further encourage the development of the pyrazole-imidazoline derivative as a hit compound using rational drug design. Anti-trypanosomatid activity was also evidenced with simple dialkyl pyrazole-3,5-dicarboxylates and their sodium salts (pyrazolates) which showed biological activity against *T. cruzi*, *L. (L.) infantum* and *L. (V.) braziliensis* by inhibition of iron superoxide dismutase [22]. Anti-*T. cruzi* activity was also recently reported for pyrazolo [3,4-e] [1,4] thiazepine with potent inhibition of CYP51 [29].

As shown in Table 1, the substitution of the imidazoline nucleus in the pyrazoles **1(a–i)** by tetrahydropyrimidine scaffold in the new series of synthetic compounds **2(a–i)**, completely abolished their trypanocidal activity, suggesting the relevance of the imidazoline ring within the molecular structure. The basicity of tetrahydropyrimidine is quite similar to that of the imidazoline ring. The nitrogen atoms at 1,3-positions are separated from each other by just one carbon atom in each heterocyclic system. The main difference regards the ring size, where the 6-membered cyclic chain shows more conformers than the 5-membered analogs; consequently, the tetrahydropyrimidine presents more flexibility than imidazoline. Since the 6-membered ring has one additional methylene group (CH_2), the hydrophobicity is greater than in the 5-membered nucleus. These molecular structural characteristics are likely to influence interactions in the drug-target binding site.

2.3. Physicochemical and ADMET properties

Although small structural changes in compounds may alter physicochemical parameters, our *in silico* prediction revealed no significant differences in physicochemical properties between **1(a–i)** and **2(a–i)** derivatives (Table 3). Both **1(a–i)** and **2(a–i)** derivatives respected Lipinski's rule of five (Ro5) as they displayed a relatively low molecular weight (MW) ≤ 320.19, low lipophilicity (cLogP ≤ 2.12 and LogD ≤ 1.26), Hydrogen-bond donors (HBDs) < 5, Hydrogen-bond acceptors (HBAs) < 10 and also low polar surface area (PSA < 79 $Å^2$) (Table 3), filling up most of the drug-likeness criteria [30]. Differences in the average of the fraction of carbons that are sp3 hybridized (Fsp3) were evidenced between series 1 (Fsp3 = 0.17) and 2 (Fsp3 = 0.23–0.29), except the derivative **1i** (Fsp3 = 0.29) (Table 3). It has been proposed that increased carbon saturation may be related to improvement in the compound's solubility, increasing the chances for success in drug discovery [31], but this concept is still controversial [32]. Neither **1(a–i)** nor **2(a–i)** series are an inducer of phospholipidosis (Table 3), suggesting no adverse effect due to accumulation of drug-phospholipid complexes in lysosomes. Interestingly, the physicochemical properties comparison of the most effective compounds, the **1c** and **1d** derivatives, and drugs that evolved to phase I of clinical trials for Chagas disease, revealed that these compounds have physical parameters (MW and cLogP) closely related to those of Bz, nifurtimox and fexinidazole, except for HBDs, HBAs and PSA, influencing intermolecular interactions, hydrophobicity, drug absorption and permeability (Fig. 1). In this context, the ADMET prediction revealed that **1c** and **1d**, as well as Bz, are more likely to be permeable to blood-brain barrier (BBB) and human intestinal absorption (Table S1). Regarding permeability in Caco-2 cells, a positive absorption was predicted only for compounds **1c** and **1d**. With respect to drug metabolism, the **1c** and **1d** derivatives are inhibitors of CYP450 1A2, which metabolizes xenobiotics and endogenous compounds such as steroid hormones [33]. In contrast to Bz, **1(a–i)** and **2(a–i)** derivatives have low risk of cardiotoxicity (weak inhibitor of hERG potassium channels), mutagenicity (no induction of Ames mutation) and carcinogenicity (Table S1).

Table 3
In silico Physicochemical parameters of pyrazole-imidazoline 1(a-i) and pyrazole-tetrahydropyrimidine 2(a-i) derivatives.

Compounds	Physicochemical properties									
	MW	logP	logD	logSw	tPSA	HBD	HBA	Solubility	Phospholipidosis	Fsp3
1a	227.27	0.5	0.05	−1.7	69.84	3	5	Good	NonInducer	0.17
1b	261.71	1.13	0.66	−2.31	69.84	3	5	Good	NonInducer	0.17
1c	296.16	1.76	1.26	−2.92	69.84	3	5	Good	NonInducer	0.17
1d	296.16	1.76	1.26	−2.92	69.84	3	5	Good	NonInducer	0.17
1e	261.71	1.13	0.66	−2.31	69.84	3	5	Good	NonInducer	0.17
1f	245.26	0.6	0.2	−1.88	69.84	3	5	Good	NonInducer	0.17
1g	306.16	1.2	0.82	−2.63	69.84	3	5	Good	NonInducer	0.17
1h	306.16	1.2	0.82	−2.63	69.84	3	5	Good	NonInducer	0.17
1i	257.29	0.48	−0.1	−1.78	69.84	3	6	Good	NonInducer	0.29
2a	241.29	0.86	−0.47	−1.99	69.84	3	5	Good	NonInducer	0.23
2b	275.74	1.49	0.13	2.6	69.84	3	5	Good	NonInducer	0.29
2c	310.18	2.12	0.74	−3.21	69.84	3	5	Good	NonInducer	0.23
2d	310.18	2.12	0.74	−3.21	69.84	3	5	Good	NonInducer	0.23
2e	275.74	1.49	0.13	2.6	69.84	3	5	Good	NonInducer	0.29
2f	259.28	0.96	−0.33	−2.17	69.84	3	5	Good	NonInducer	0.29
2g	320.19	1.55	0.3	−2.92	69.84	3	5	Good	NonInducer	0.29
2h	320.19	1.55	0.3	−2.92	79.07	3	5	Good	NonInducer	0.29
2i	271.32	0.83	−0.63	2.07	69.84	3	6	Good	NonInducer	0.29

MW - Molecular weight: logP - The logarithm of the partition coefficient between n-octanol and water, characterizing lipophilicity; logD - Represents the logP of compounds at physiological pH (7.4); logSw - represents the logarithm of compounds water solubility computed by the ESOL method; tPSA - Topological Polar Surface Area; HBD - Hydrogen Bond Donnors; HBA - Hydrogen Bond Acceptors; Solubility - Water Solubility estimated by Hill method; Fsp3 - Fraction of sp3 carbon.

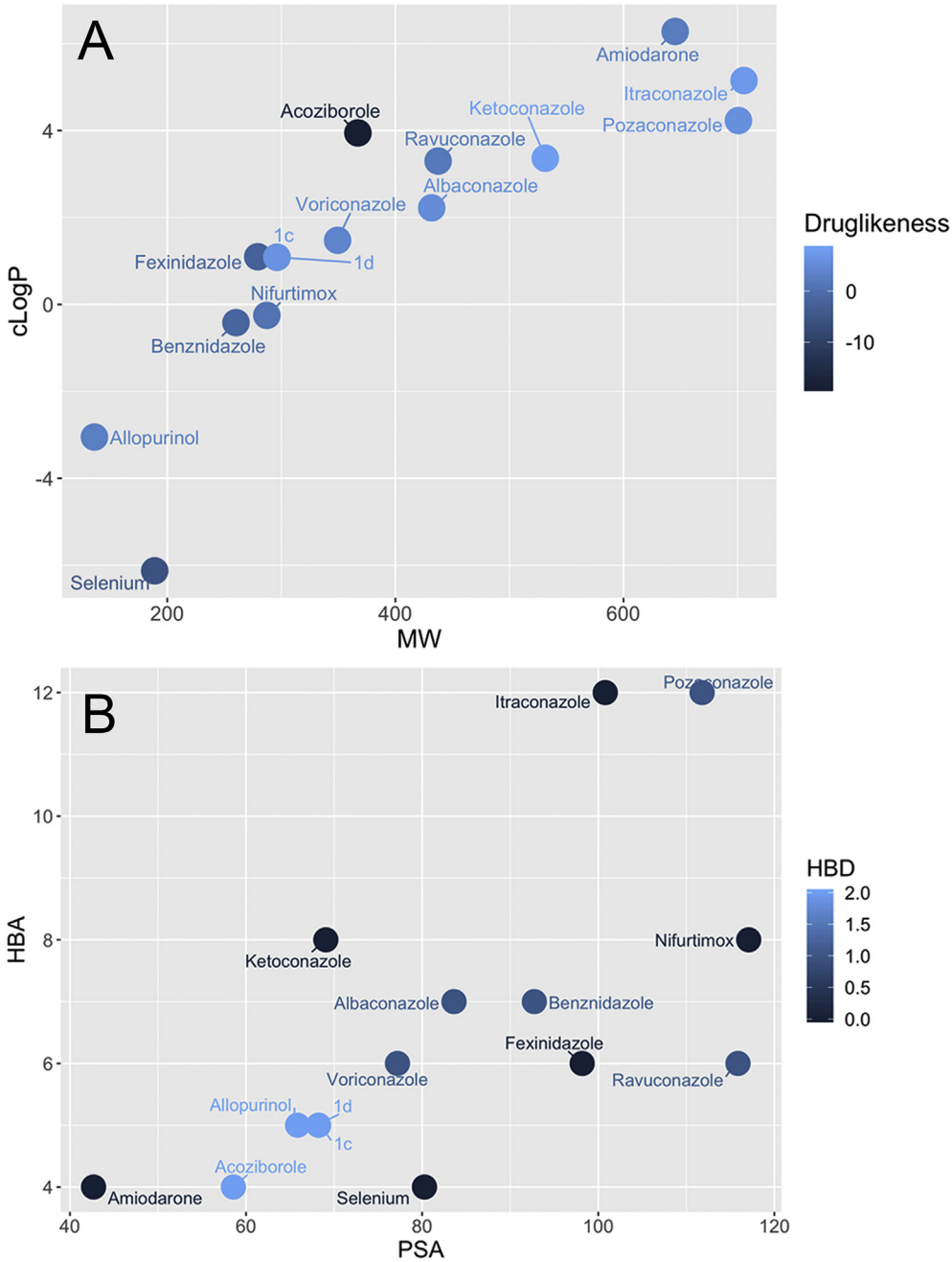

Fig. 1. Physicochemical properties of compounds **1c** and **1d** and drugs used to treat Chagas disease that advance at least to phase I clinical trials. (A) Comparison of molecular weight (MW) and lipophilicity (cLogP), color scale represents drug-likeness. (B) Distribution of drugs based on hydrogen bond acceptors (HBA) and topological surface area (PSA); color scale represents hydrogen bond donors (HBD). Physicochemical properties were calculated using DataWarrior software and graphics were created using R. (For interpretation of the references to color in this figure legend, the reader is referred to the Web version of this article).

2.4. Structure-activity relationship (SAR) analysis

The impact of modifications in the benzene ring associated with pyrazole-imidazoline derivatives was evaluated by the structure-activity relationship analysis (SAR). Compound optimization was performed by addition of halogens, in different positions of the benzene ring, and methoxy group (*para*-position) in both pyrazole-imidazoline and pyrazole-tetrahydropyrimidine series. The results highlight the influence of the chlorine atom in the biological activity of the pyrazole-imidazoline derivatives (Fig. 2). Dichlorinated derivatives, **1c** and **1d**, were more effective than monochlorinateds, **1b** and **1e,** against intracellular amastigotes (Dm28c-Luc). Potency was preserved when two chlorine atoms at two *meta*-positions (**1c**; $IC_{50} = 16.5 \pm 1.6\ \mu M$) were switched between the *meta*- and *para*-positions (**1d**; $IC_{50} = 13.6 \pm 1.5\ \mu M$). In monochlorinated compounds, the substitution of chlorine in the *meta*-to *para*-position induced loss of activity. Replacement of chorine atom at *para*-position by other halogens, bromine and fluorine, or methoxy group reduced the activity of the compounds (Fig. 2). Switching the chlorine (**1b**) for bromine (**1h**) atom at *meta*-position and also methoxy group at *para*-position reduced approximately 3-fold the trypanocidal activity. Curiously, all compounds with halogens,

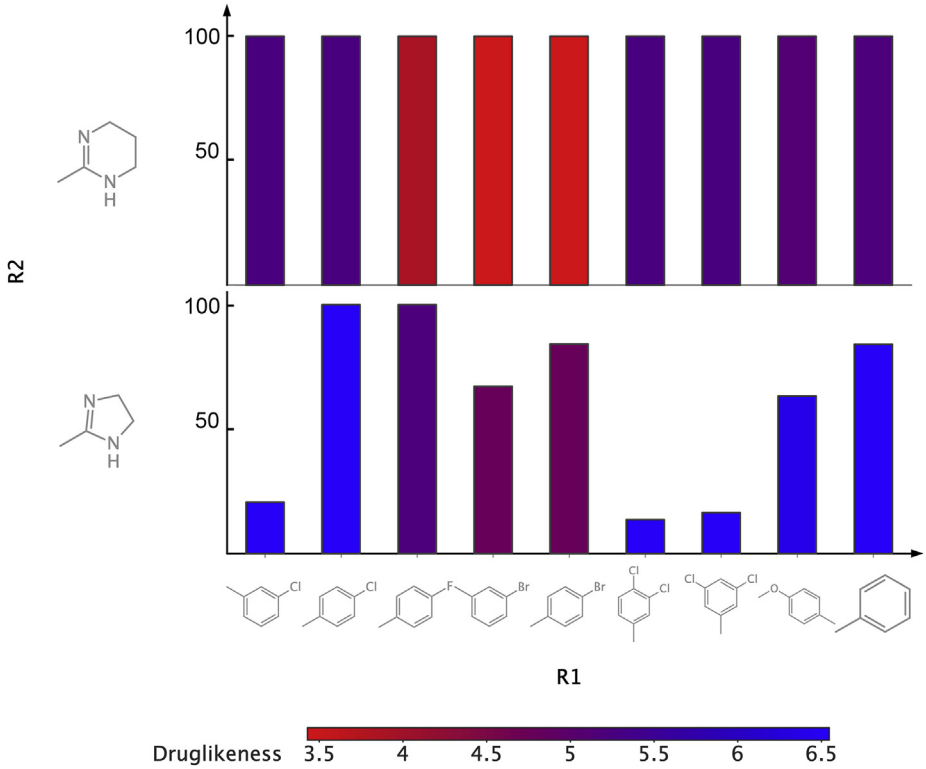

Fig. 2. Structure-activity relationship (SAR) analysis of pyrazole-imidazoline and pyrazole-tetrahydropyrimidine derivatives. The amino-pyrazole center was used to separate substituents in R1 (halogen and methoxy group insertions and position in benzene ring) and R2 (imidazoline or tetrahydropyrimidine rings). Bars represent mean values of IC_{50} achieved against intracellular amastigotes; color scale denotes the drug-likeness of each compound. Chlorine-containing compounds of pyrazole-imidazoline derivatives (**1b-d**) at meta-position were the most active compounds of the series. (For interpretation of the references to color in this figure legend, the reader is referred to the Web version of this article).

including chlorine atom, and methoxy group at *para*-position of the benzene ring linked to pyrazole-imidazoline derivatives showed low trypanocidal activity ($IC_{50} \geq 63.3\ \mu M$), except for *meta*- and *para*-position of dichloride derivative (**1d**; $IC_{50} = 13.6 \pm 1.5\ \mu M$). Overall, these data suggest that chlorination at the *meta*-position may be crucial to the enhancement of trypanocidal activity by pyrazole-imidazoline derivatives. In contrast, the electronic influences of the halogen and methoxy substituents did not result in an increase of potency of pyrazole-tetrahydropyrimidine derivatives (Fig. 2), suggesting a steric rather than an electronic effect. The role of the halogen bond has been highlighted in drug discovery, with organohalogens achieving 34% of pre- or clinical trials stages [34]. But even though chlorine atom has been prominent as a promoter of biological activity, chlorination may also abolish drug activity or induce toxicological properties [35].

2.5. In silico drug-target search

Subsequent analyses were performed to identify possible binding targets for **1(a–i)** and **2(a–i)** compounds. Computational analyses using DataWarrior software were based on the available data of trypanocidal compounds integrated into Chembl database. A total of 34.154 compounds were identified with activity against 16 targets of *T. cruzi*, including 6-phospho-1-fructokinase, bifunctional dihydrofolate reductase-thymidylate synthase, cruzipain, cyclic nucleotide specific phosphodiesterase, deoxyuridine triphosphatase, farnesyl diphosphate synthase, farnesyl synthetase, farnesyltransferase, glyceraldehyde-3-phosphate dehydrogenase, glycosomal hexokinase, spermidine synthase, sterol 14-alpha demethylase, trans-sialidase, triosephosphate isomerase, trypanothione reductase and tubulin alpha chain. Next, the compounds' scaffolds were queried in this small library of compounds using the core-based SAR analysis tool available in the program, which identified 302 molecules, with activity $\leq 10\ \mu M$, containing the selected fragments (Fig. 3). Only 2 targets of *T. cruzi*, 6-phospho-1-fructokinase and cruzipain, were spotted by compounds containing the selected fragments in their structures (Fig. 3). Notably, cruzipain, the major cysteine proteinase of *T. cruzi* that belongs to the papain-like clan CA, was the most recorded target in this set of compounds. Pyrazole and imidazoline scaffolds were identified in 93.7% and 2.6%, respectively, of the total active compounds identified for cruzipain after fragment-based screening (Fig. 3). Only few compounds containing pyrazole scaffold (0.09%) identified 6-phospho-1-fructokinase in the library (Fig. 3). Although the pyrazole-tetrahydropyrimidine derivatives have not been active, 11 tetrahydropyrimidine-containing compounds capable of recognizing cruzipain are registered in the chembl database, suggesting that the tetrahydropyrimidine scaffold may influence pharmacological activity when linked to a heterocyclic compounds such as thiophene, imidazole or furan [36].

Cruzipain has been highlighted as an important target for drug design due to its relevance in parasite metabolism and survival [37]. Cruzipain is expressed in all development stages of *T. cruzi* and its inhibition leads to blockage of parasite invasion [38], metacyclogenesis and intracellular development [39]. K777 (N-[(2 S)-1-[[(E,3 S)-1-(benzenesulfonyl)-5-phenylpent-1-en-3-yl]amino]-1-oxo-3-phenylpropan-2-yl]-4-methylpiperazine-1-carboxamide, an irreversible vinyl sulfone cruzipain inhibitor, showed potent efficacy in preclinical trials, validating cruzipain as a potential chemotherapeutic target [40,41]. Tetrafluorophenoxy ketone

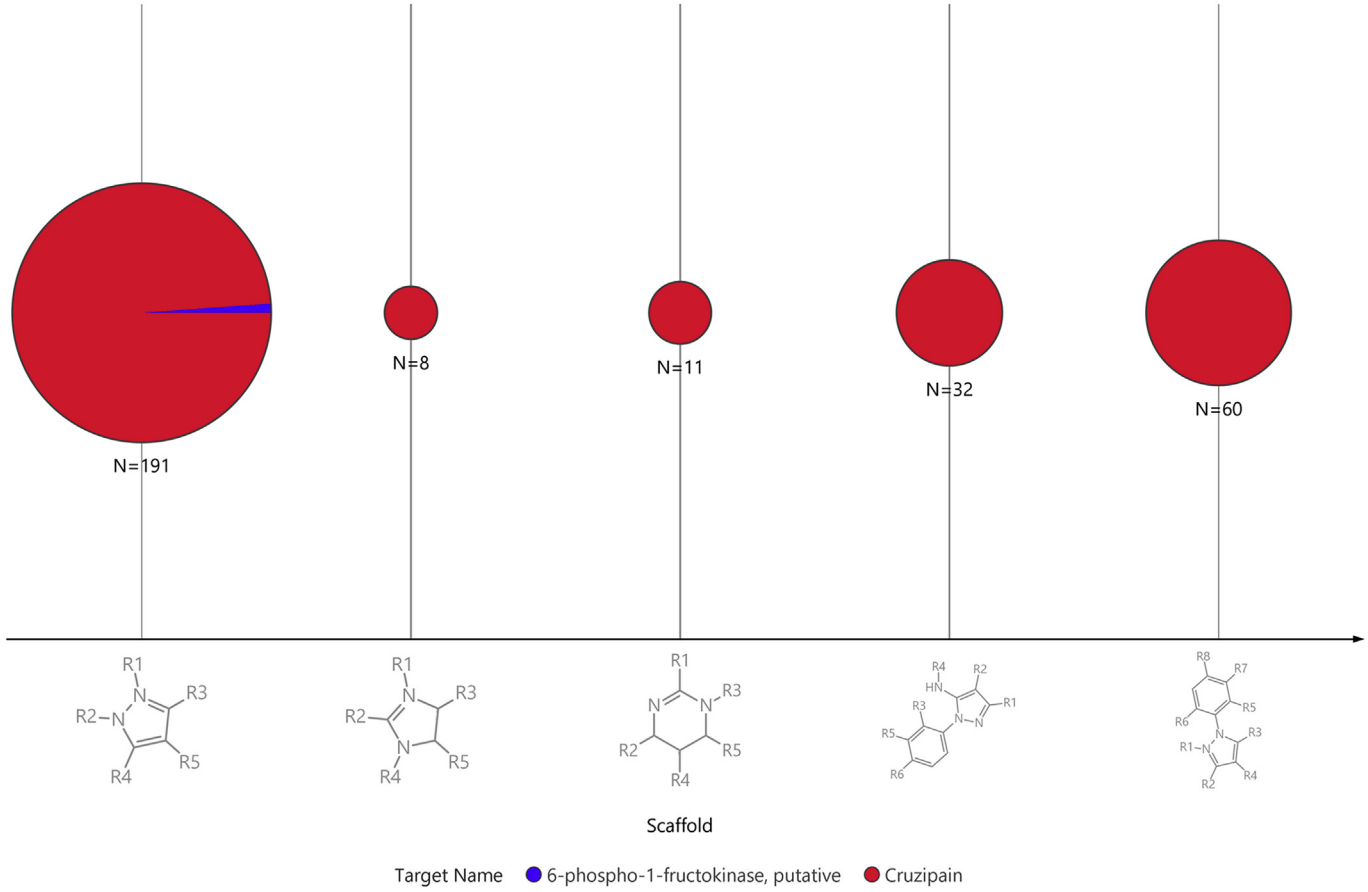

Fig. 3. *In silico* fragment-based search of molecular scaffolds. Matched scaffolds of pyrazole-imidazoline and pyrazole-tetrahydropyrimidine to trypanocidal compounds with activity (≤10 μM), against annotated targets in Chembl database. Analysis were made using DataWarrior software and retrieved two *T. cruzi* targets, cruzipain and putative 6-phospho-1-fructokinase, N represents the number of compounds with each matched scaffold. (For interpretation of the references to color in this figure legend, the reader is referred to the Web version of this article).

analogs have also been identified as promising cruzipain inhibitors, showing trypanocidal activity in a mouse model of acute *T. cruzi* infection [42]. Optimization of tetrafluorophenoxy ketone by addition of the pyrazolopyrimidine ring potentially improved trypanocidal activity and oral bioavailability [43]. Additionally, pyrazole derivatives, such as N-(1H-benzimidazol-2-yl)-1,3-dimethyl-pyrazole-4-carboxamide (PDB code: 4W5B) [44] and N-(1H-benzimidazol-2-yl)-3-(4-fluorophenyl)-1H-pyrazole-4-carboxamide (PDB code: 4W5C) [45], also bind to cruzipain and have been considered promising *T. cruzi* chemotherapeutic agents. Accordingly, we docked compounds **1c** and **1d** in the 4W5B cruzipain active site to predict binding poses and interactions between cruzipain and pyrazole-imidazoline derivatives.

2.6. Prediction of compounds binding-mode

Compound N-(1*H*-benzimidazol-2-yl)-1,3-dimethyl-pyrazole-4-carboxamide (3H5) from the 4W5B protein data base (PDB) file was used as default and compared with **1c** and **1d** derivatives. In the initial stage of these experiments, 4W5B redocking assays were performed under both rigid and flexible binder conditions and with protonation of the active center histidine residue. The rigid 3H5 linker: deprotonated histidine −7.85 kcal/mol and RMSD 1.15 Å; histidine protonated −7.85 kcal/mol and RMSD 1.3 Å. The flexible 3H5 linker: deprotonated histidine −7.54 kcal/mol and RMSD 3.5 Å; histidine protonated −7.85 kcal/mol and RMSD 1.3 Å (Fig. S1). In this way, for the subsequent docking tests we adopted the ligand flexible configuration with the residue and histidine protonated. Docking results showed that the compound **1c** ligand presented a score −7.7 kcal/mol and RMSD 4.0 Å, and the **1d** ligand had a score −7.8 kcal/mol and RMSD 4.4 Å.

The binding modes of the crystallized complexes as 4W5B, 3iut and 3kku with their respective 3H5, KB2 and B95 ligands, were analyzed and the amino acid residues, that participate in the binding site with the different ligands, identified. This analysis allowed us to recognize that different ligands crystallized in the active site of cruzipain have common binding residues in PDBs 4W5B, 3uit and 3kku including GLY23, CYS25, GLY65, GLY66, ASP161, HIS162 and GLY163 (Fig. 4). We also noticed that the residues of TRP26, LEU67 and LEU160 perform interactions only with 3uit and 3kku available in PDB while GLN19 with 3uit and 4W5B in PDB. Except for LEU67 and LEU160, we have estimated that the remaining amino acid residues also interact with the compounds **1c** and **1d**.

Through the docking assays, we observed that the complexes of the PDB files and the docked compounds showed hydrophobic bonds with amino acid residues at the active site of cruzipain (Fig. 4). In addition, the chlorine atom of both compounds possibly binds to amino acids residues, **1c** interacts with SER35 residue, while **1d** chlorine atoms closely pose to GLY66 and SER35 in active site of the enzyme by hydrogen bond of 2.8 Å. This finding suggests that chlorine atoms may contribute favorably to the stability of the

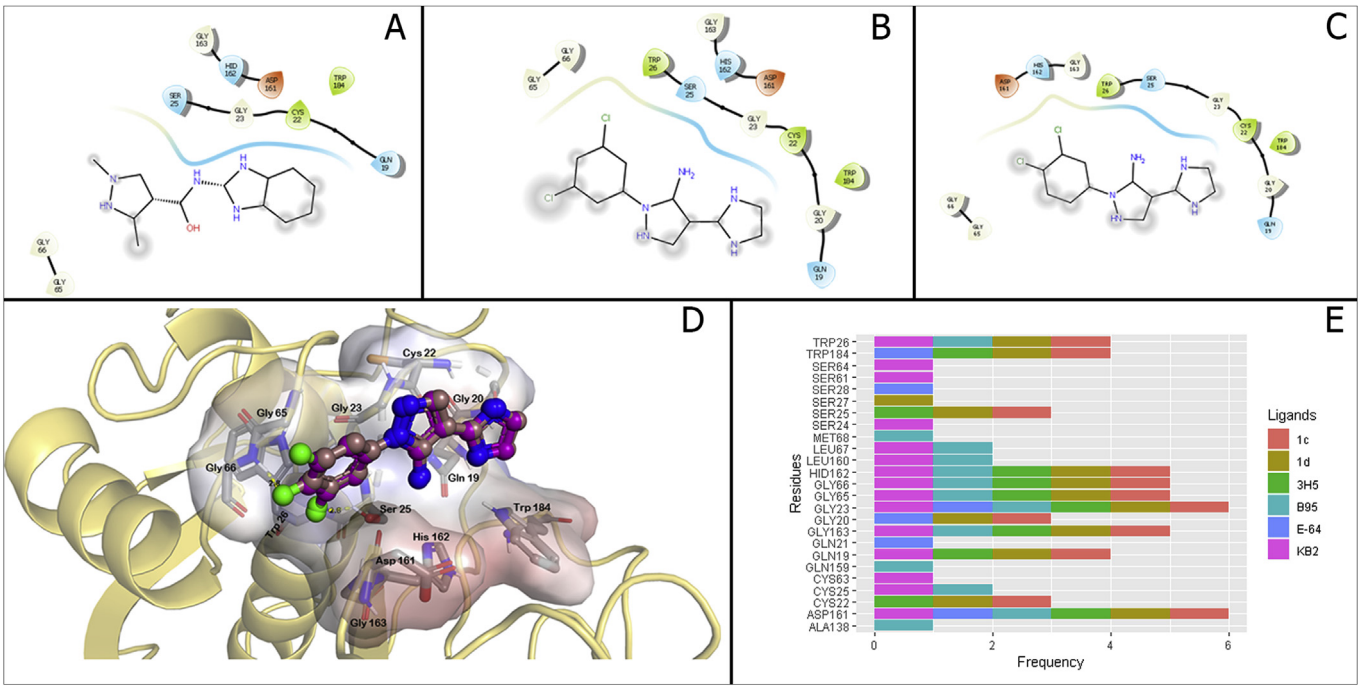

Fig. 4. Molecular docking analysis of **1c**, **1d** and inhibitors of cruzipain into enzyme binding pocket. (A) Binding mode of 3H5 [1 (N-(1*H*-benzimidazol-2-yl)-1,3-dimethyl-pyrazole-4-carboxamide)](PDB: 4W5B), compounds **1c** (B) and **1d** (C), showing hydrophobic (gray) interactions with amino acid residues inside cruzipain active site. (D) Docking analysis of **1c** and **1d** binding poses, showing that compounds interact mostly with the same residues and are tightly superimposed. The residues GLY66 and SER65 interact closely (2.8 Å) to chlorine atoms of **1d**, whereas, only Ser65 interact with chlorine atom at para position in **1c**. (E) Mapping of important amino acid residues in binding pocket of cruzipain crystallographic structures available in PDB 4W5B, 3IUT and 3KKU. Mapping performed considering interactions with respective ligands 3H5, KB2 and B95, compound **1c**, **1d** and E-64, a cysteine protease inhibitor. Most common residues that interact with ligands in cruzipain active site are GLY23, GLY65, GLY66, ASP161, HIS162 and GLY163. Docking visualization of binding poses and amino acid residue interactions were performed using PyMOL and Maestro (Schrödinger). (For interpretation of the references to color in this figure legend, the reader is referred to the Web version of this article).

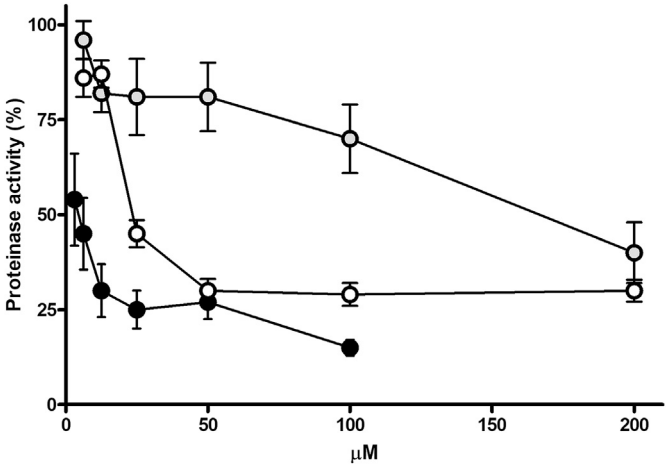

Fig. 5. Proteinase activities of *Trypanosoma cruzi* trypomastigotes proteins extract. For the enzyme quantification, about 5 μg of the protein was incubated with 30 μM of Z-FR-AMC, in enzyme activation buffer pH 5.0, at 37 °C. The activities of the samples were followed by co-incubation with different concentrations (μM) of E-64 (black circle), **1c** (white circle) and **1d** (gray circle) compounds. Results presented as percentile of proteinase activity (%) and represent the median of three analyses. In these assays, 100% of activity is relative to 88×10^5 μmol min^{-1} mg of protein^{-1}.

ligand-target complex at the binding site of cruzipain, a property that is also exploited for some experimental and approved drugs in clinical development [46].

For comparison purposes, the binding mode of E-64, a classical inhibitor of cysteine proteinase, was accessed (−7.0 kcal/mol). The results also indicated the partitioning of GLY23 and ASP161 residues of the enzyme in the interaction with this compound. Among the 33 compounds identified in the virtual screening, 4 compounds (Flucloxacillin sodium, Cefoperazone sodium, Piperacillin sodium, Etofyllin clofibrate), which interact with the catalytic amino acids SER25, HIS162 and TRP184, were identified as potential inhibitors of cruzipain [47].

Thus, considering the binding prediction for **1c** and **1d** in the active site of cruzipain, an open question was whether this mainly hydrophobic interaction could lead to inhibition of the cysteine proteinase activity of *T. cruzi*. In this way, we performed a kinetics of the enzymatic activity using a fluorogenic substrate. The results indicated that **1c** and **1d** derivatives inhibit cysteine proteinase activity from *T. cruzi* protein extract, assessed with Z-FR-AMC that is an excellent substrate for the fluorometric assay of cysteine proteinase [48]. The inhibition rate reached levels of 50% enzymatic activity (44×10^5 μmol min^{-1} mg of protein^{-1}) with 24 μM and 180 μM for **1c** and **1d** derivatives, respectively. Compared with the IC_{50} value of E-64 (3.0 μM), an irreversible and selective inhibitor of cysteine proteinase [49], the **1c** and **1d** compounds showed a lower performance of 8-fold and 60-fold, respectively. (Fig. 5). Interestingly, although derivatives **1c** and **1d** have similar anti-*T. cruzi* activity, they have quite distinct inhibitory activity for cysteine protease. The difference between enzymatic activity and trypanocidal effect suggests that these derivatives may act as a multi-target drug. Further studies will be conducted to evaluate the multi-target profile of both derivatives and also their inhibitory activity of purified *T. cruzi* cruzipain for molecular docking validation.

Pyrazole derivatives have been described as inhibitors of iron superoxide dismutase (65–98% inhibition) [50] and CYP51 ($IC_{50} = 0.1$ μM) [29] of *T. cruzi* and reported as potential anti-cathepsin B, H and L agents [51]. Hybrid compounds based on

1,4-dihydropyridine and pyrazole moieties showed potential antimalarial activity against chloroquine-sensitive *Plasmodium falciparum*, whose falcipain-2 inhibition, a plasmodial cysteine proteinase, was proposed as mechanism of action [52]. These data highlight that the structural optimization of pyrazole derivatives may contribute to the identification of novel antiparasitic drugs.

3. Conclusion

Chagas disease chemotherapy remains an important challenge. Only two drugs, each with significant limitations of efficacy and presenting serious adverse effects, are currently used in the clinic for treatment of Chagas disease. The identification of effective and safe new drugs is essential to bring hope to millions of chronically infected individuals, most with severe cardiomyopathies. Here, we integrated *in silico* analyses and preclinical *in vitro* assays to evaluate the trypanocidal activity and predict drug-likeness properties and drug-target interactions. *In vitro* phenotypical screening and SAR analysis revealed the effectiveness of two dichlorinated pyrazole-imidazoline derivatives, compounds **1c** and **1d**, against *T. cruzi*, highlighting the influence of the chlorine atom at the *meta*-position of the benzene ring in the compound's potency. These compounds showed important physicochemical properties similar to chemotherapeutic clinical agents (benznidazole and nifurtimox) and also to drugs that advanced to phase I clinical trials. Structure-based virtual screening predicted cruzipain as a potential biological target of pyrazole-imidazoline derivatives. Theoretical evaluation of the docking complexes revealed that both compounds (1**c** and 1**d**) have potential to bind to the active site of cruzipain as a cysteine proteinase inhibitor of *T. cruzi*, highlighting them as promising novel drug candidates for the control of Chagas disease.

4. Material and methods

4.1. Compounds

All commercial reagents were used as received unless otherwise noted. The reaction progress was monitored by thin layer chromatography (TLC) with precoated 60 F254 silica gel plates. The melting points were determined on a Fisatom 430 apparatus. Infrared spectra (FT-IR) were recorded on a PerkinElmer Spectrum 100, ATR diamond-ZnSe apparatus, wave numbers expressed in cm^{-1}. NMR spectra were recorded on a Bruker Avance (500 or 400 MHz), at 298 K, in $CDCl_3$, methanol-d_4 or DMSO-d_6. Chemical shifts (δ) are expressed in parts per million (ppm) and coupling constants (J) in Hertz (Hz). The High-Resolution Mass Spectrometry (HRMS) was performed using Micromass/Waters ZQ-4000 Spectrometer, capillary 3.0 kV, cone 30.0 V, extrator 1 V, RF lens 1.0 V, source temperature 150 °C, desolvation temperature 300 °C (Electrospray Ionization-ESI). The key intermediates 5-amino-1-aryl-1*H*-pyrazole-4-carbonitriles **4(a–i)** were synthesized by our research group according to described previously.

4.1.1. General procedure for synthesis of 5-amino-1-aryl-4-(4,5-dihydro-1H-imidazol-2-yl)-1H-pyrazoles ***1(a–i)***

5-amino-1-aryl-1*H*-pyrazole-4-carbonitriles **4(a–i)** (0.001 mol), 2.0 mL of 1,2-diaminoethane (ethylenediamine) and carbon disulfide (0.004 mol) were added into a 50 mL round-bottom flask adapted with a glass condenser. The mixture was kept at 110-115°C for 12-14 hours. After that, the productwas poured into cold water, the precipitate was filtered out and washed with cold water. The reactions were accompanied by means of TLC and dichloromethane as eluent.

*4.1.1.1. 5-amino-4-(4,5-dihydro-1H-imidazol-2-yl)-1-phenyl-1H-pyrazole (**1a**).* Yield: 55%; mp: 138–140 °C; FT-IR ν (cm^{-1}): 3351, 3264, 3149, 3074, 934, 2885, 2864, 1595, 1567; ^{1}H NMR (500 MHz, MeOH-d$_4$): $\delta = 7.69$ (s, 1H), 7.53–7.54 (m, 4H), 7.42–7.45 (m, 1H), 3.65 (s, 4H); ^{13}C NMR (125 MHz, MeOH-d$_4$): $\delta = 162.8$, 148.9, 140.1, 139.4, 130.8, 129.4, 125.6, 95.6, 49.8; HRMS (ESI): m/z [M+H]$^+$: calcd. for $C_{12}H_{13}N_5$: 228.1249; found: 228.1261.

*4.1.1.2. 5-amino-1-(3-chlorophenyl)-4-(4,5-dihydro-1H-imidazol-2-yl)-1H-pyrazole (**1b**).* Yield: 74%; mp: 160–162 °C; FT-IR ν (cm^{-1}): 3376, 3280, 3222, 3171, 2948, 2922, 2876, 1632, 1609, 1594, 1569; ^{1}H NMR (500 MHz, MeOH-d$_4$): $\delta = 7.70$ (s, 1H), 7.61–7.62 (m, 1H), 7.52–7.53 (m, 2H), 7.42–7.44 (m, 1H), 3.65 (s, 4H); ^{13}C NMR (125 MHz, MeOH-d$_4$): $\delta = 162.7$, 149.1, 140.7, 140.6, 136.2, 132.1, 129.1, 125.4, 123.4, 96.0; HRMS (ESI): m/z [M+H]$^+$: calcd. for $C_{12}H_{12}ClN_5$: 262.0859; found: 262.0877.

*4.1.1.3. 5-amino-1-(3,5-dichlorophenyl)-4-(4,5-dihydro-1H-imidazol-2-yl)-1H-pyrazole (**1c**).* Yield: 83%; mp: 96–98 °C; FT-IR ν (cm^{-1}): 3420, 3282, 3083, 2946, 2873, 1619, 1583, 1568; ^{1}H NMR (500 MHz, DMSO-d_6): $\delta = 7.76$ (s, 1H), 7.67 (d, $J = 1.8$ Hz, 2H), 7.62 (t, $J = 1.8$ Hz, 1H), 6.85 (br, 2H), 3.53 (s, 4H); ^{13}C NMR (125 MHz, DMSO-d_6): $\delta = 160.1$, 148.6, 140.8, 140.2, 135.0, 126.7, 121.6, 94.6, 48.3; HRMS (ESI): m/z [M+H]$^+$: calcd. for $C_{12}H_{11}Cl_2N_5$: 296.0470; found: 296.0474.

*4.1.1.4. 5-amino-1-(3,4-dichlorophenyl)-4-(4,5-dihydro-1H-imidazol-2-yl)-1H-pyrazole (**1d**).* Yield: 71%; mp: 197–199 °C; FT-IR ν (cm^{-1}): 3418, 3298, 3074, 2935, 2873, 1611, 1560, 1522; ^{1}H NMR (500 MHz, DMSO-d_6): $\delta = 7.85$ (d, $J = 2.5$ Hz, 1H), 7.78 (d, $J = 8.7$ Hz, 1H), 7.73 (s, 1H), 7.63 (dd, $J = 8.7$, 2.5 Hz, 1H), 6.77 (br, 2H), 3.51 (s, 4H); ^{13}C NMR (125 MHz, DMSO-d_6): $\delta = 159.8$, 147.9, 139.2, 138.3, 131.6, 131.1, 128.8, 124.0, 122.5, 94.8; HRMS (ESI): m/z [M+H]$^+$: calcd. for $C_{12}H_{11}Cl_2N_5$: 296.0470; found: 296.0472.

*4.1.1.5. 5-amino-1-(4-chlorophenyl)-4-(4,5-dihydro-1H-imidazol-2-yl)-1H-pyrazole (**1e**).* Yield: 42%; mp: 179–181 °C; FT-IR ν (cm^{-1}): 3397, 3265, 3122, 2932, 2852, 1606, 1568, 1523; ^{1}H NMR (500 MHz, MeOH-d$_4$): $\delta = 7.69$ (s, 1H), 7.54 (s, 4H), 3.65 (s, 4H); ^{13}C NMR (125 MHz, MeOH-d$_4$): $\delta = 162.6$, 148.9, 140.3, 138.0, 134.7, 130.8, 126.8, 95.8, 49.7; HRMS (ESI): m/z [M+H]$^+$: calcd. for $C_{12}H_{12}ClN_5$: 262.0859; found: 262.0861.

*4.1.1.6. 5-amino-4-(4,5-dihydro-1H-imidazol-2-yl)-1-(4-fluorophenyl)-1H-pyrazole (**1f**).* Yield: 66%; mp: 164–166 °C; FT-IR ν (cm^{-1}): 3280, 3075, 2943, 2872,1611, 1598, 1567; ^{1}H NMR (500 MHz, MeOH-d$_4$): $\delta = 7.68$ (s, 1H), 7.55 (dd, $J = 9.0$, 4.8 Hz, 2H), 7.28 (t, $J = 9.0$ Hz, 2H), 3.65 (s, 4H); ^{13}C NMR (125 MHz, MeOH-d$_4$): $\delta = 163.6$ (d, $J = 244.2$ Hz), 162.5, 149.0, 140.1, 135.5 (d, $J = 2.9$ Hz), 127.9 (d, $J = 8.9$ Hz), 117.4 (d, $J = 23.3$ Hz), 95.6, 49.7; HRMS (ESI): m/z [M+H]$^+$: calcd. for $C_{12}H_{12}FN_5$: 246.1155; found: 246.1162.

*4.1.1.7. 5-amino-1-(4-bromophenyl)-4-(4,5-dihydro-1H-imidazol-2-yl)-1H-pyrazole (**1g**).* Yield: 84%; mp: 184–188 °C; FT-IR ν (cm^{-1}): 3387, 3260, 3119, 2926, 2852, 1605, 1566, 1523; ^{1}H NMR (400 MHz, MeOH-d$_4$): $\delta = 7.68$–7.70 (m, 3H), 7.49 (d, $J = 8.9$ Hz, 2H), 3.65 (s, 4H); ^{13}C NMR (100 MHz, MeOH-d$_4$): $\delta = 161.1$, 147.5, 138.9, 137.1, 132.4, 125.6, 121.1, 94.2; HRMS (ESI): m/z [M+H]$^+$: calcd. for $C_{12}H_{12}BrN_5$: 306.0354; found: 306.0365.

*4.1.1.8. 5-amino-1-(3-bromophenyl)-4-(4,5-dihydro-1H-imidazol-2-yl)-1H-pyrazole (**1h**).* Yield: 47%; mp: 88–92 °C; FT-IR ν (cm^{-1}): 3442, 3321, 3249, 3088, 3063, 2941, 2869, 1614, 1592, 1527; ^{1}H NMR (400 MHz, MeOH-d$_4$): $\delta = 7.76$ (t, $J = 1.9$ Hz, 1H), 7.70 (s, 1H), 7.56–7.60 (m, 2H), 7.45 (t, $J = 8.0$ Hz, 1H), 3.65 (s, 4H); ^{13}C NMR

(100 MHz, MeOH-d_4): $\delta = 161.1$, 147.6, 139.2, 139.1, 130.7, 130.6, 126.7, 122.3, 122.3, 94.4; HRMS (ESI): m/z $[M+H]^+$: calcd. for $C_{12}H_{12}BrN_5$: 306.0354; found: 306.0357.

*4.1.1.9. 5-amino-4-(4,5-dihydro-1H-imidazol-2-yl)-1-(4-methoxyphenyl)-1H-pyrazole (**1i**).* Yield: 50%; mp: 171–173 °C; FT-IR ν (cm^{-1}): 3263, 2940, 2857, 2837, 1602, 1561, 1510; ^{1}H NMR (500 MHz, MeOH-d_4): $\delta = 7.65$ (s, 1H), 7.41 (d, $J = 8.9$ Hz, 2H), 7.07 (d, $J = 8.9$ Hz, 2H), 3.85 (s, 3H), 3.64 (s, 4H); ^{13}C NMR (125 MHz, MeOH-d4): $\delta = 162.8$, 161.1, 148.8, 139.6, 131.8, 127.4, 115.8, 95.3, 56.1, 49.7; HRMS (ESI): m/z $[M+H]^+$: calcd. for $C_{13}H_{15}N_5O$: 258.1355; found: 258.1366.

*4.1.2. General procedure for synthesis of 2-(-5-amino-1-aryl-1H-pyrazol-4-yl)-1,4,5,6-tetrahydropyrimidines **2(a–i)***

The experimental procedure was similar to synthesis of analogs **1(a–i)**. 5-amino-1-aryl-1*H*-pyrazole-4-carbonitriles **4(a–i)** (0.001 mol) were reacted with 2.0 mL of 1,3-diaminopropane and carbon disulfide (0.004 mol). The temperature was 85-95°C and the reaction time was 14-16 hours. The reaction mixture was poured into cold water, the precipitate was filtered out and washed with cold water. The reactions were accompanied by means of TLC and dichloromethane as eluent.

*4.1.2.1. 2-(5-amino-1-phenyl)-1H-pyrazol-4-yl)-1,4,5,6-tetrahydropyrimidine (**2a**).* Yield: 48%; mp:146–147 °C; FT-IR ν (cm^{-1}): 3313, 3184, 3039, 2972, 2876, 1612, 1596, 1556, 1529. ^{1}H NMR (400 MHz, MeOD) $\delta = 7.71$ (s, 1H), 7.55–7.57 (m, 4H), 7.39 (s, 1H), 3.49 (t, $J = 5.7$ Hz, 4H), 1.95 (quint, $J = 5.7$ Hz, 2H). ^{13}C NMR (100 MHz, MeOD) $\delta = 154.8$, 148.8, 140.2, 139.0, 131.3, 129.5, 124.4, 99.8, 41.7, 21.4. HRMS (ESI): m/z $[M+H]^+$: calcd. for $C_{13}H_{16}N_5$: 242.1406; found: 242.1413.

*4.1.2.2. 2-(5-amino-1-(3-chlorophenyl)-1H-pyrazol-4-yl)-1,4,5,6-tetrahydropyrimidine (**2b**).* Yield: 56%; mp: 130–132 °C; FT-IR ν (cm^{-1}): 3306, 3260, 3194, 2962, 2869, 1611, 1594, 1552, 1533; ^{1}H NMR (400 MHz, MeOH-d_4) $\delta = 7.71$ (s, 1H), 7.59–7.60 (m, 1H), 7.51–7.52 (m, 2H), 7.45–7.46 (m, 1H), 3.49 (t, $J = 5.8$ Hz, 4H), 1.96 (quint, $J = 5.8$ Hz, 2H); ^{13}C NMR (100 MHz, MeOH-d_4) $\delta = 155.0$, 148.7, 140.4, 140.3, 136.3, 132.1, 129.5, 125.8, 123.9, 41.3, 21.0; HRMS (ESI): m/z $[M+H]^+$: calcd. for $C_{13}H_{14}ClN_5$: 276.1016; found: 276.1022.

*4.1.2.3. 2-(5-amino-1-(3,5-dichlorophenyl)-1H-pyrazol-4-yl)-1,4,5,6-tetrahydropyrimidine (**2c**).* Yield: 64%; mp: 144 °C; FT-IR ν (cm^{-1}): 3306, 3078, 3048, 2941, 2860, 1610, 1585, 1569, 1522; ^{1}H NMR (400 MHz, $CDCl_3$) $\delta = 7.56$ (d, $J = 1.8$ Hz, 2H), 7.50 (s, 1H), 7.32 (t, $J = 1.8$ Hz, 1H), 4.13 (br, 2H), 3.45 (t, $J = 5.8$ Hz, 4H), 1.86 (quint, $J = 5.8$ Hz, 2H); ^{13}C NMR (100 MHz, $CDCl_3$) $\delta = 151.1$, 146.9, 140.4, 137.2, 136.0, 127.3, 121.5, 99.8, 41.8, 21.4; HRMS (ESI): m/z $[M+H]^+$: calcd. for $C_{13}H_{13}Cl_2N_5$: 310,0626; found: 310.0634.

*4.1.2.4. 2-(5-amino-1-(3,4-dichlorophenyl)-1H-pyrazol-4-yl)-1,4,5,6-tetrahydropyrimidine (**2d**).* Yield: 77%; mp: 188–190 °C; FT-IR ν (cm^{-1}): 3448, 3296, 3230, 3068, 2936, 2860, 1621, 1595, 1555, 1501; ^{1}H NMR (400 MHz, MeOH-d_4) $\delta = 7.78$ (d, $J = 2.4$ Hz, 1H), 7.67–7.68 (m, 2H), 7.54 (dd, $J = 8.7$, 2.4 Hz, 1H), 3.42 (t, $J = 5.8$ Hz, 4H), 1.87 (quint, $J = 5.8$ Hz, 2H); ^{13}C NMR (100 MHz, MeOH-d_4) $\delta = 154.4$, 148.8, 139.8, 139.3, 134.3, 132.6, 132.5, 127.0, 124.7, 100.5, 42.3, 22.0; HRMS (ESI): m/z $[M+H]^+$: calcd. for $C_{13}H_{13}Cl_2N_5$: 310.0626; found: 310.0636.

*4.1.2.5. 2-(5-amino-1-(4-chlorophenyl)-1H-pyrazol-4-yl)-1,4,5,6-tetrahydropyrimidine (**2e**).* Yield: 50%; mp: 164–168 °C; FT-IR ν (cm^{-1}): 3314, 3215, 3087, 2941, 2862, 2840, 1603, 1579, 1560, 1521; ^{1}H NMR (400 MHz, MeOH-d_4) $\delta = 7.64$ (s, 1H), 7.53 (s, 4H), 3.40 (t, $J = 5.8$ Hz, 4H), 1.84 (quint, $J = 5.8$ Hz, 2H); ^{13}C NMR (100 MHz, MeOH-d_4) $\delta = 152.8$, 147.0, 137.7, 136.8, 133.1, 129.3, 125.3, 99.0, 40.8, 20.6; HRMS (ESI): m/z $[M+H]^+$: calcd. for $C_{13}H_{14}ClN_5$: 276.1016; found: 276.1025.

*4.1.2.6. 2-(5-amino-1-(4-fluorophenyl)-1H-pyrazol-4-yl)-1,4,5,6-tetrahydropyrimidine (**2f**).* Yield: 5%; mp: 146–147 °C; FT-IR ν (cm^{-1}): 3392, 3281, 3098, 2951, 2936, 2855, 1610, 1593, 1567, 1532; ^{1}H NMR (400 MHz, $CDCl_3$) $\delta = 7.50$–7.54 (m, 3H), 7.17 (t, $J = 8.3$ Hz, 2H), 3.46 (t, $J = 5.8$ Hz, 4H), 1.87 (quint, $J = 5.8$ Hz, 2H); ^{13}C NMR (100 MHz, $CDCl_3$) $\delta = 161.9$ (d, $J = 248.0$ Hz), 151.4, 146.6, 136.5, 134.5 (d, $J = 2.9$ Hz), 125.9 (d, $J = 8.6$ Hz), 116.7 (d, $J = 22.9$ Hz), 99.0, 41.6, 21.3; HRMS (ESI): m/z $[M+H]^+$: calcd. for $C_{13}H_{14}FN_5$: 260.1311; found: 260.1319.

*4.1.2.7. 2-(5-amino-1-(4-bromophenyl)-1H-pyrazol-4-yl)-1,4,5,6-tetrahydropyrimidine (**2g**).* Yield: 42%; mp: 192–198 °C; FT-IR ν (cm^{-1}): 3411, 3225, 3098, 2951, 2934, 2850, 1610, 1575, 1560, 1511; ^{1}H NMR (400 MHz, MeOH-d_4) $\delta = 7.69$ (s, 1H), 7.66 (d, $J = 8.8$ Hz, 2H), 7.47 (d, $J = 8.8$ Hz, 2H), 3.42 (t, $J = 5.8$ Hz, 4H), 1.88 (quint, $J = 5.8$ Hz, 2H). ^{13}C NMR (100 MHz, MeOH-d_4) $\delta = 154.5$, 148.4, 139.4, 138.5, 133.8, 127.1, 122.5, 99.6, 41.9, 21.7; HRMS (ESI): m/z $[M+H]^+$: calcd. for $C_{13}H_{14}BrN_5$: 320.0511; found: 320.0520.

*4.1.2.8. 2-(5-amino-1-(3-bromophenyl)-1H-pyrazol-4-yl)-1,4,5,6-tetrahydropyrimidine (**2h**).* Yield: 52%; mp: 100–104 °C; FT-IR ν (cm^{-1}): 3250, 3103, 3063, 2951, 2865, 2825, 1605, 1590, 1532; ^{1}H NMR (400 MHz, MeOH-d_4) $\delta = 7.74$ (t, $J = 1.9$ Hz, 1H), 7.69 (s, 1H), 7.54–7.60 (m, 2H), 7.42–7.45 (m, 1H), 3.48 (t, $J = 5.8$ Hz, 4H), 1.95 (quint, $J = 5.8$ Hz, 2H); ^{13}C NMR (100 MHz, MeOD): $\delta = 155.0$, 140.5, 136.5, 132.4, 131.8, 130.9, 128.7, 125.6, 121.5, 99.7, 41.4, 21.1; HRMS (ESI): m/z $[M+H]^+$: calcd. for $C_{13}H_{14}BrN_5$: 320.0511; found: 320.0517.

*4.1.2.9. 2-(5-amino-1-(4-methoxyphenyl)-1H-pyrazol-4-yl)-1,4,5,6-tetrahydropyrimidine (**2i**).* Yield: 45%; mp: 177–179 °C; FT-IR ν (cm^{-1}): 3310, 3245, 3092, 2942, 2863, 2848, 1603, 1578, 1550, 1532; ^{1}H NMR (400 MHz, MeOD) $\delta = 7.68$ (s, 1H), 7.42 (d, $J = 8.8$ Hz, 2H), 7.10 (d, $J = 8.8$ Hz, 2H), 3.87 (s, 3H), 3.48 (t, $J = 5.8$ Hz, 4H), 1.95 (quint, $J = 5.8$ Hz, 2H). ^{13}C NMR (100 MHz, MeOD): $\delta = 162.0$, 155.1, 148.4, 137.8, 132.3, 127.4, 115.8, 99.5, 55.7, 41.7; 21.2; HRMS (ESI): m/z $[M+H]^+$: calcd. for $C_{14}H_{17}N_5O$: 272.1511; found: 272.1520.

4.2. Cell cultures

Vero cells (ATCC® CCL81™), derived from the kidney of an African green monkey, were subcultured with dissociation solution (0.25% trypsin-EDTA) when cultures achieved 80–100% confluence. Subsequently, the cells were washed and cultivated in RPMI-1640 medium with 10% fetal bovine serum (FBS).

Primary cultures of heart muscle cells were obtained from 18 days mouse fetuses as previously described [53]. Ventricular tissue was dissociated with trypsin and collagenase type II solution. Isolated cells were cultivated in Dulbecco's modified Eagle medium, supplemented with 7% fetal FBS, 2% chicken embryo extract, 1 mM L-glutamine and antibiotics, and maintained at 37 °C in 5% CO_2 atmosphere. All procedures with experimental animals were approved by the Institutional Animal Care and Utilization Committee (license L15-17).

4.3. Parasites

Bloodstream trypomastigote forms of *T. cruzi*, Y strain (TcII), were obtained by cardiac puncture of *Swiss webster* infected mice at

the parasitemia peak (7° days post infection; dpi). Tissue culture-derived trypomastigotes, Dm28c-Luc clone (genetically modified to express the firefly luciferase) (TcI), were harvested from infected Vero cells cultures supernatants at 4° dpi. The selection of the *T. cruzi* lineages, TcI and TcII, is related to their frequent association with human infection. All animal procedures were approved by the institutional ethics committee (license L15-17).

4.4. Parasite protein extraction and quantification

Trypomastigotes of *T. cruzi* (1×10^8) were washed three times by centrifugation (3500 g, 10 min, 4 °C) in PBS (pH 7.2) and then subjected to 4 cycles of vortex-mixing for 30 min in lysis buffer (100 mM Tris-HCl pH 8.0, 150 mM NaCl, 10% glycerol, 0.6% Triton X-100). The soluble protein fraction was obtained by centrifugation (25,000 g, 30 min, 4 °C) and stored (−20 °C) until further use. Protein concentration was determined by colorimeter assay as previously described [54], using BSA as standard protein.

4.5. Proteinase activity in solution

The proteinase activities of parasite proteins (5 μg), which was used as positive activity control, were accessed in activation buffer [CH_3COONa 10 mM, pH 5.0 containing 1 mM DTT, final volume of 100 μL], using fluorogenic peptide substrates [30 μM N-benzyloxycarbonyl-L-phenylalanyl-L-arginine 7-amino-4-methylcoumarin (Z-FR-AMC)]. Samples were incubated for 45 min at 37 °C, and the variance in the relative fluorescence units was monitored with a spectrophotometer SpectraMaxM2^e (Molecular Devices). Inhibition assays were performed by coincubation with different concentration of the compounds (**1c** and **1d**) and transepoxysuccinyl-L-leucylamido-(4-guanidino)butane (E-64) separately. The substrate cleavage rate was defined as follow: $v = \Delta s/\Delta t$, where v = velocity, Δs = substrate concentration variation and Δt = total reaction time [55]. The assays were controlled verifying the self-degradation of the fluorescent peptide substrate at the same time interval. The releasing amount of Amino Methyl Coumarin during the reaction was calculated by using a Molar Extinction Coefficient ($\varepsilon = 1.78 \times 10^4\ M^{-1}\ cm^{-1}$). Additional control was performed at low concentration (≤1%) of dimethyl sulfoxide (DMSO). The enzymatic activity is expressed as μmol min^{-1} mg of $protein^{-1}$.

4.6. Cytotoxicity assay

Vero cells, seeded in 96-well white culture plates at a density of 1.5×10^4 cells/well, were used to analyze the toxic effect of pyrazole derivatives to mammalian cells. Twenty-four hours later, cells were exposed to a range of Bz and pyrazole analogs concentration (1.95–500 μM) for 72 h at 37 °C. CellTiter-Glo kit (Promega Corporation, Madison, WI, USA) was used to evaluate cell viability based on ATP measurement and luminescent signal was read on FlexStation 3 reader (Molecular Devices, Sunnyvale, CA, USA). The most active compounds against *T. cruzi* were further evaluated for cardiotoxicity. Thus, primary cultures of heart muscle cells (5×10^4 cells/well) were also applied in the viability assays after treatment with the most effective compounds. The concentration of compound that reduces 50% of mammalian cell viability (CC_{50}) was determined by linear regression. Control was performed at low concentration (≤1%) of dimethyl sulfoxide (DMSO). At least three independent assays were performed in duplicate.

4.7. Antiparasitic assay

Screening of active compounds against *T. cruzi* was performed on trypomastigotes and intracellular amastigotes, relevant forms in human infection. Trypomastigotes (1×10^6 parasites/well), Y strain and Dm28c-Luc clone, were treated for 24 h at 37 °C with the pyrazole derivatives and Bz at different concentrations (0.41–100 μM). Viable parasites of *T. cruzi* Y strain were measured by ATP-based quantification usig CellTiter Glo whereas for clone Dm28c-Luc the viability was determined by the activity of the enzyme luciferase [56]. The luminescent signal was detected in the FlexStation 3 reader. The IC_{50} and IC_{90} values (concentration capable of reducing the number of viable parasites by 50% and 90%, respectively) was calculated by linear regression. Bz and DMSO (concentration ≤1%) were used as positive and negative controls, respectively.

The susceptibility of intracellular amastigotes to compounds was first tested on Vero cells infected with *T. cruzi* Dm28c-Luc clone (10:1 parasites/host cell). *T. cruzi*-infected cultures (24 h) were treated for 72 h at 37 °C with serial dilution of pyrazole derivatives and Bz (0.41–100 μM). Intracellular amastigotes viability, evaluated by addition of luciferin (300 μg/mL), was analyzed using FlexStation 3 reader. Effective compounds were also screened against *T. cruzi*-infected heart muscle cells (Y strain; 72 h). After staining with Giemsa, the IC_{50} and IC_{90} values of compounds were determined by counting intracellular amastigotes and infected cells under optical microscope. A minimum of three independent experiments were performed in duplicate.

4.8. Physicochemical and ADMET prediction

Physicochemical properties associated with compounds were calculated using Datawarrior software version 4.7.3 [36] and FAFDrugs4 (http://fafdrugs4.mti.univ-paris-diderot.fr/). For target search Datawarrior was used to retrieve molecules within ChEMBL database annotated to target *T. cruzi* proteins. Compounds were filtered by IC_{50} and potency (≤10 μM), any duplicity were removed, then, fragments of pyrazole-imidazoline and pyrazole-tetrahydropyrimidine were queried against the small library of compounds. ADMET parameters (adsorption, distribution, metabolism, elimination and toxicity) were acquired inserting compounds molecular structures in ADMETsar plataform (http://lmmd.ecust.edu.cn/admetsar1).

4.9. Molecular docking

The binding mode of **1c** and **1d** compounds into *T. cruzi* cysteine proteinase were assessed by docking using the DockThor program [57,58]. The crystal structure of cruzipain complexed with 3H5 compound [1 (N-(1H-benzimidazol-2-yl)-1,3-dimethyl-pyrazole-4-carboxamide)] was obtained from the Protein Data Bank (PDB accession number 4W5B). The docking was established in a cubic grid box of 10 by 10 by 10 Å3, and the parameters are referred to as defaults in DockThor. Structures with positional root mean square deviation (RMSD) of up to 2 Å were clustered together, and the results with the most favorable free energy of binding were selected as the resultant complex structures. We also performed redocking of 3H5 to the crystal structure of cruzipain, with a success rate (RMSD of 2.0 Å for the interface backbone atoms) of 53%. The docking assays were repeated three times.

Acknowledgements

The authors thank the Multi-user Research Facility of Bioassay Platform of Instituto Oswaldo Cruz, Fiocruz, Rio de Janeiro, Brazil. This work was supported by research funds from the Oswaldo Cruz Institute of the Oswaldo Cruz Foundation (Fiocruz), Programa Estratégico de Apoio à Pesquisa em Saúde (Papes VI)/Conselho Nacional de Desenvolvimento Científico e Tecnológico (CNPq), Brazil (grant 421856/2017-3 and 424015/2018-8 to M.C.S.P.),

Fundação de Amparo à Pesquisa do Estado do Rio de Janeiro (FAPERJ) (grant E-26/010.001548/2014 and E-26/110.553/2014 to M.C.S.P.) and Coordenação de Aperfeiçoamento de Pessoal de Nível Superior - Brasil (CAPES) - Finance Code 001. This work is a collaboration research project of members of the Rede Mineira de Química (RQ-MG) supported by FAPEMIG-Brazil (Project: CEX-RED-00010-14 to M.S.) and Programa Primeiros Projetos (Project: CEX-APQ-01014-14 to M.S.). We thank The Program for Technological Development in Tools for Health-RPT-Fiocruz for use of its facilities.

Appendix A. Supplementary data

Supplementary data to this article can be found online at https://doi.org/10.1016/j.ejmech.2019.111610.

References

[1] World Health Organization, Chagas disease (American trypanosomiasis) Fact sheet, 2017. Available in, http://www.who.int/mediacentre/factsheets/fs340/en/.
[2] J.C. Dias, A.N. Ramos Jr., E.D. Gontijo, A. Luquetti, M.A. Shikanai-Yasuda, J.R. Coura, R.M. Torres, J.R. Melo, E.A. Almeida, W. Oliveira Jr., A.C. Silveira, J.M. Rezende, F.S. Pinto, A.W. Ferreira, A. Rassi, A.A. Fragata Filho, A.S. Sousa, D. Correia Filho, A.M. Jansen, G.M. Andrade, C.F. Britto, A.Y. Pinto, A. Rassi Jr., D.E. Campos, F. Abad-Franch, S.E. Santos, E. Chiari, A.M. Hasslocher-Moreno, E.F. Moreira, D.S. Marques, E.L. Silva, J.A. Marin-Neto, L.M. Galvão, S.S. Xavier, S.A. Valente, N.B. Carvalho, A.V. Cardoso, R.A. Silva, V.M. Costa, S.M. Vivaldini, S.M. Oliveira, V.D. Valente, M.M. Lima, R.V. Alves, Brazilian consensus on Chagas disease, Epidemiol. Serv. Saude. 25 (2015) 7–86, 2016.
[3] E.E. Conners, J.M. Vinetz, J.R. Weeks, K.C. Brouwer, A global systematic review of Chagas disease prevalence among migrants, Acta Trop. 156 (2016) 68–78.
[4] A. Rassi Jr., A. Rassi, J. Marcondes de Rezende, American trypanosomiasis (Chagas disease), Infect. Dis. Clin. N. Am. 26 (2012) 275–291.
[5] F.R. Martins-Melo, A.N. Ramos Jr., C.H. Alencar, J. Heukelbach, Mortality from neglected tropical diseases in Brazil, 2000-2011, Bull. World Health Organ. 94 (2016) 103–110.
[6] B.Y. Lee, S.M. Bartsch, L. Skrip, D.L. Hertenstein, C.M. Avelis, M. Ndeffo-Mbah, C. Tilchin, E.O. Dumonteil, A. Galvani, Are the London declaration's 2020 goals sufficient to control Chagas disease?: modeling scenarios for the Yucatan Peninsula, PLoS Neglected Trop. Dis. 12 (2018), e0006337.
[7] E. Pinheiro, L. Brum-Soares, R. Reis, J.C. Cubides, Chagas disease: review of needs, neglect, and obstacles to treatment access in Latin America, Rev. Soc. Bras. Med. Trop. 50 (2017) 296–300.
[8] E. Chatelain, Chagas disease research and development: is there light at the end of the tunnel? Comput. Struct. Biotechnol. J. 15 (2016) 98–103.
[9] I. Molina, J. Gómez i Prat, F. Salvador, B. Treviño, E. Sulleiro, N. Serre, D. Pou, S. Roure, J. Cabezos, L. Valerio, A. Blanco-Grau, A. Sánchez-Montalvá, X. Vidal, A. Pahissa, Randomized trial of posaconazole and benznidazole for chronic Chagas' disease, N. Engl. J. Med. 370 (2014) 1899–1908.
[10] C.A. Morillo, H. Waskin, S. Sosa-Estani, M. Del Carmen Bangher, C. Cuneo, R. Milesi, M. Mallagray, W. Apt, J. Beloscar, J. Gascon, I. Molina, L.E. Echeverria, H. Colombo, J.A. Perez-Molina, F. Wyss, B. Meeks, L.R. Bonilla, P. Gao, B. Wei, M. McCarthy, S. Yusuf, STOP-CHAGAS Investigators, Benznidazole and posaconazole in eliminating parasites in asymptomatic *T. cruzi* carriers: the STOP-CHAGAS trial, J. Am. Coll. Cardiol. 69 (2017) 939–947.
[11] C.A. Morillo, J.A. Marin-Neto, A. Avezum, S. Sosa-Estani, A. Rassi Jr., F. Rosas, E. Villena, R. Quiroz, R. Bonilla, C. Britto, F. Guhl, E. Velazquez, L. Bonilla, B. Meeks, P. Rao-Melacini, J. Pogue, A. Mattos, J. Lazdins, A. Rassi, S.J. Connolly, S. Yusuf, BENEFIT Investigators, Randomized trial of benznidazole for chronic Chagas' cardiomyopathy, N. Engl. J. Med. 373 (2015) 1295–1306.
[12] Drugs for neglected disease initiative (DNDi) fexinidazole (Chagas), 2018. https://www.dndi.org/diseases-projects/portfolio/fexinidazole-chagas/.
[13] M.J. Alam, O. Alam, P. Alam, M.J. Naim, A review on pyrazole chemical entity and biological activity, Int. J. Pharma Sci. Res. 6 (2015) 1433–1442.
[14] A. Ansari, A. Ali, M. Asifa, Shamsuzzaman, Review: biologically active pyrazole derivatives, New J. Chem. 41 (2017) 16–41.
[15] J.V. Faria, P.F. Vegi, A.G.C. Miguita, M.S. Santos, N. Boechat, A.M.R. Bernardino, Recently reported biological sctivities of pyrazole compounds, Bioorg. Med. Chem. 25 (2017) 5891–5903.
[16] K. Karrouchi, S. Radi, Y. Ramli, J. Taoufik, Y.N. Mabkhot, F.A. Al-Aizari, M. Ansar, Synthesis and pharmacological activities of pyrazole derivatives: a review, Molecules 23 (2018) E134.
[17] A.A. Bekhit, A.M. Hassan, H.A. Abd El Razik, M. M El-Miligy, E.J. El-Agroudy, Ael-D. Bekhit, New heterocyclic hybrids of pyrazole and its bioisosteres: design, synthesis and biological evaluation as dual acting antimalarial-antileishmanial agents, Eur. J. Med. Chem. 94 (2015) 30–44.
[18] S. Brand, N.R. Norcross, S. Thompson, J.R. Harrison, V.C. Smith, D.A. Robinson, L.S. Torrie, S.P. McElroy, I. Hallyburton, S. Norval, P. Scullion, L. Stojanovski, F.R. Simeons, D. van Aalten, J.A. Frearson, R. Brenk, A.H. Fairlamb, M.A. Ferguson, P.G. Wyatt, I.H. Gilbert, K.D. Read, Lead optimization of a pyrazole sulfonamide series of *Trypanosoma brucei* N-myristoyltransferase inhibitors: identification and evaluation of CNS penetrant compounds as potential treatments for stage 2 human African trypanosomiasis, J. Med. Chem. 57 (2014) 9855–9869.
[19] N. Kumar, S. Sreenivasa, V. Kumar, N.R. Mohan, 3-(3,5-Difluorophenyl)-1-phenyl-1H-pyrazole-4-carbaldehyde, Molbank 3 (2018) M1011.
[20] H. Liu, Z.L. Ren, W. Wang, J.X. Gong, M.J. Chu, Q.W. Ma, J.C. Wang, X.H. Lv, Novel coumarin-pyrazole carboxamide derivatives as potential topoisomerase II inhibitors: design, synthesis and antibacterial activity, Eur. J. Med. Chem. 157 (2018) 81–87.
[21] A.B. Vaidya, J.M. Morrisey, Z. Zhang, S. Das, T.M. Daly, T.D. Otto, N.J. Spillman, M. Wyvratt, P. Siegl, J. Marfurt, G. Wirjanata, B.F. Sebayang, R.N. Price, A. Chatterjee, A. Nagle, M. Stasiak, S. Charman, I. Angulo-Barturen, S. Ferrer, M. Belén Jiménez-Díaz, M.S. Martínez, F.J. Gamo, V.M. Avery, A. Ruecker, M. Delves, K. Kirk, M. Berriman, S. Kortagere, J. Burrows, E. Fan, L.W. Bergman, Pyrazoleamide compounds are potent antimalarials that target Na+ homeostasis in intraerythrocytic *Plasmodium falciparum*, Nat. Commun. 5 (2014) 5521.
[22] F. Reviriego, F. Olmo, P. Navarro, C. Marín, I. Ramírez-Macías, E. García-España, M.T. Albelda, R. Gutiérrez-Sánchez, M. Sánchez-Moreno, V.J. Arán, Simple dialkyl pyrazole-3,5-dicarboxylates show in vitro and in vivo activity against disease-causing trypanosomatids, Parasitol 144 (2017) 1133–1143.
[23] M. Krasavin, Biologically active compounds based on the privileged 2-imidazoline scaffold: the world beyond adrenergic/imidazoline receptor modulators, Eur. J. Med. Chem. 97 (2015) 525–537.
[24] S.K. Sharma, P. Kumar, B. Narasimhan, K. Ramasamy, V. Mani, R.K. Mishra, A.B.A. Majeed, Synthesis, antimicrobial, anticancer evaluation and QSAR studies of 6-methyl-4- [1-(2-substituted-phenylamino-acetyl)-1H-indol-3-yl]-2-oxo/thioxo-1,2,3,4 tetrahydropyrimidine-5-carboxylic acid ethyl esters, Eur. J. Med. Chem. 48 (2012) 16–25.
[25] C.H. Ríos Martínez, F. Miller, K. Ganeshamoorthy, F. Glacial, M. Kaiser, H.P. de Koning, A.A. Eze, L. Lagartera, T. Herraiz, C. Dardonville, A new nonpolar N-hydroxy imidazoline lead compound with improved activity in a murine model of late-stage *Trypanosoma brucei brucei* infection is not cross-resistant with diamidines, Antimicrob. Agents Chemother. 59 (2015) 890–904.
[26] I.O. Donkor, H. Assefa, D. Rattendi, S. Lane, M. Vargas, B. Goldberg, C. Bacchi, Trypanocidal activity of dicationic compounds related to pentamidine, Eur. J. Med. Chem. 36 (2001) 531–538.
[27] M.S. Santos, M.L. Oliveira, A.M. Bernardino, R.M. de Léo, V.F. Amaral, F.T. de Carvalho, L.L. Leon, M.M. Canto-Cavalheiro, Synthesis and antileishmanial evaluation of 1-aryl-4-(4,5-dihydro-1H-imidazol-2-yl)-1H-pyrazole derivatives, Bioorg. Med. Chem. Lett 21 (2011) 7451–7454.
[28] M.S. Santos, A.M.R. Bernardino, L.C.S. Pinheiro, M.M. Canto-Cavalheiro, L. Leon, An efficient synthesis of new 5-(1-aryl-1H-pyrazole-4-yl)-1H-tetrazoles from 1-aryl-1H-pyrazole-4-carbonitriles via [3 + 2] cycloaddition reaction, J. Heterocycl. Chem. 49 (2012) 1425–1428.
[29] L.F.A. Fiuza, R.B. Peres, M.R. Simões-Silva, P.B. da Silva, D.D.G.J. Batista, C.F. da Silva, A. Nefertiti Silva da Gama, T.R. Krishna Reddy, M.N.C. Soeiro, Identification of Pyrazolo[3,4-e][1,4]thiazepin based CYP51 inhibitors as potential Chagas disease therapeutic alternative: in vitro and in vivo evaluation, binding mode prediction and SAR exploration, Eur. J. Med. Chem. 149 (2018) 257–268.
[30] D. Lagorce, D. Douguet, M.A. Miteva, B.O. Villoutreix, Computational analysis of calculated physicochemical and ADMET properties of protein-protein interaction inhibitors, Sci. Rep. 7 (2017) 46277.
[31] F. Lovering, J. Bikker, C. Humblet, Escape from flatland: increasing saturation as an approach to improving clinical success, J. Med. Chem. 52 (2009) 6752–6756.
[32] D. Muthas, S. Boyer, C. Hasselgren, A critical assessment of modeling safety-related drug attrition, Med. Chem. Commun. 7 (2013) 1058–1065.
[33] J. Ren, G.G. Chen, Y. Liu, X. Su, B. Hu, B.C. S Leung, Y. Wang, R.L.K. Ho, S. Yang, G. Lu, C.G. Lee, P.B. S Lai, Cytochrome P450 1A2 metabolizes 17β-estradiol to suppress hepatocellular carcinoma, PLoS One 11 (2016), e0153863.
[34] Z. Xu, Z. Yang, Y. Liu, Y. Lu, K. Chen, W. Zhu, Halogen bond: its role beyond drug-target binding affinity for drug discovery and development, J. Chem. Inf. Model. 54 (2014) 69–78.
[35] K. Naumann, How chlorine in molecules affects biological activity, Euro Chlor (2003) 1–31.
[36] T. Sander, J. Freyss, M. von Korff, R.C. DataWarrior, An open-source program for chemistry aware data visualization and analysis, J. Chem. Inf. Model. 55 (2015) 460–473.
[37] V.G. Duschak, A.S. Couto Cruzipain, The major cysteine protease of *Trypanosoma cruzi*: a sulfated glycoprotein antigen as relevant candidate for vaccine development and drug target, Curr. Med. Chem. 16 (2009) 3174–3202.
[38] J. Scharfstein, V. Schmitz, V. Morandi, M.M. Capella, A.P. Lima, A. Morrot, L. Juliano, W. Müller-Esterl, Host cell invasion by *Trypanosoma cruzi* is potentiated by activation of bradykinin B(2) receptors, J. Exp. Med. 192 (2000) 1289–1300.
[39] B.M. Cazzulo, J. Martínez, M.J. North, G.H. Coombs, J.J. Cazzulo, Effects of proteinase inhibitors on the growth and differentiation of *Trypanosoma cruzi*, FEMS Microbiol. Lett. 124 (1994) 81–86.
[40] J.C. Engel, P.S. Doyle, I. Hsieh, J.H. McKerrow, Cysteine protease inhibitors cure an experimental *Trypanosoma cruzi* infection, J. Exp. Med. 188 (1998) 725–734.
[41] P.S. Doyle, Y.M. Zhou, J.C. Engel, J.H. McKerrow, A cysteine protease inhibitor

cures Chagas' disease in an immunodeficient-mouse model of infection, Antimicrob. Agents Chemother. 51 (2007) 3932–3939.
[42] K. Brak, I.D. Kerr, K.T. Barrett, N. Fuchi, M. Debnath, K. Ang, J.C. Engel, J.H. McKerrow, P.S. Doyle, L.S. Brinen, J.A. Ellman, Nonpeptidic tetrafluorophenoxymethyl ketone cruzain inhibitors as promising new leads for Chagas disease chemotherapy, J. Med. Chem. 53 (2010) 1763–1773.
[43] R.J. Neitza, C. Bryanta, S. Chena, J. Guta, E.H. Casellia, S. Poncea, S. Chowdhuryb, H. Xub, M.R. Arkina, J.A. Ellmanb, A.R. Rensloa, Tetrafluorophenoxymethyl ketone cruzain inhibitors with improved pharmacokinetic properties as therapeutic leads for Chagas' disease, Bioorg. Med. Chem. Lett 25 (2015) 4834–4837.
[44] PDB, Available online, http://www.rcsb.org/pdb/explore.do?structureId=4w5b. accessed on 31 October 2018.
[45] PDB, Available online, https://www.rcsb.org/structure/4W5C. accessed on 3 January 2019.
[46] M.Z. Hernandes, S.M. Cavalcanti, D.R. Moreira, W.F. de Azevedo Junior, A.C. Leite, Halogen atoms in the modern medicinal chemistry: hints for the drug design, Curr. Drug Targets 11 (2010) 303–314.
[47] I. Palos, E.E. Lara-Ramirez, J.C. Lopez-Cedillo, C. Garcia-Perez, M. Kashif, V. Bocanegra-Garcia, B. Nogueda-Torres, G. Rivera, Repositioning FDA drugs as potential cruzain inhibitors from *Trypanosoma cruzi*: virtual screening, in vitro and in vivo studies, Molecules 22 (2017) E1015.
[48] A.J. Barrett, Fluorimetric assays for cathepsin B and cathepsin H with methylcoumarylamide substrates, Biochem. J. 187 (1980) 909–912.
[49] A.J. Barrett, A.A. Kembhavi, M.A. Brown, H. Kirschke, C.G. Knight, M. Tamai, K. Hanada, L-trans-Epoxysuccinyl-leucylamido(4-guanidino)butane (E-64) and its analogues as inhibitors of cysteine proteinases including cathepsins B, H and L, Biochem. J. 201 (1982) 189–198.
[50] M. Sánchez-Moreno, C. Marín, P. Navarro, L. Lamarque, E. García-España, C. Miranda, O. Huertas, F. Olmo, F. Gómez-Contreras, J. Pitarch, F. Arrebola, In vitro and in vivo trypanosomicidal activity of pyrazole-containing macrocyclic and macrobicyclic polyamines: their action on acute and chronic phases of Chagas disease, J. Med. Chem. 55 (2012) 4231–4243.
[51] N. Raghav, M. Singh, SAR studies of some acetophenone phenylhydrazone based pyrazole derivatives as anticathepsin agents, Bioorg. Chem. 75 (2017) 38–49.
[52] P. Kumar, K. Kadyan, M. Duhan, J. Sindhu, V. Singh, B.S. Saharan, Design, synthesis, conformational and molecular docking study of some novel acyl hydrazone based molecular hybrids as antimalarial and antimicrobial agents, Chem. Cent. J. 11 (2017) 115–128.
[53] M.N. Meirelles, T.C. de Araujo-Jorge, C.F. Miranda, W. de Souza, H.S. Barbosa, Interaction of *Trypanosoma cruzi* with heart muscle cells: ultrastructural and cytochemical analysis of endocytic vacuole formation and effect upon myogenesis in vitro, Eur. J. Cell Biol. 41 (1986) 198–206.
[54] O.H. Lowry, N.J. Rosebrough, A.L. Farr, R.J. Randall, Protein measurement with the Folin phenol reagent, J. Biol. Chem. 193 (1951) 265–275.
[55] C.R. Alves, S. Corte-Real, S.C. Bourguignon, C.S. Chaves, E.M. Saraiva, *Leishmania amazonensis*: early proteinase activities during promastigote-amastigote differentiation in vitro, Exp. Parasitol. 109 (2005) 38–48.
[56] L.S. Lara, C.S. Moreira, C.M. Calvet, G.C. Lechuga, R.S. Souza, S.C. Bourguignon, V.F. Ferreira, D. Rocha, M.C.S. Pereira, Efficacy of 2-hydroxy-3-phenylsulfanylmethyl-[1,4]-naphthoquinone derivatives against different *Trypanosoma cruzi* discrete type units: identification of a promising hit compound, Eur. J. Med. Chem. 144 (2018) 572–581.
[57] C.S. de Magalhães, H.J.C. Barbosa, L.E. Dardenne, A genetic algorithm for the ligand-protein docking problem, Genet. Mol. Biol. 27 (2004) 605–610.
[58] F. Souza-Silva, S.C. Bourguignon, B.A. Pereira, L.M. Côrtes, L.F. de Oliveira, A. Henriques-Pons, L.C. Finkelstein, V.F. Ferreira, P.F. Carneiro, R.T. de Pinho, E.R. Caffarena, C.R. Alves, Epoxy-α-lapachone has in vitro and in vivo anti-leishmania (Leishmania) amazonensis effects and inhibits serine proteinase activity in this parasite, Antimicrob. Agents Chemother. 59 (2015) 1910–1918.